ROLE OF CIRCUMFERENTIAL FLOW IN THE STABILITY OF FLUID-HANDLING MACHINE ROTORS

D.E. Bently and A. Muszynska
Bently Rotor Dynamics Research Corporation
Minden, Nevada 89423, U.S.A.

The recent studies of the dynamic stiffness properties of fluid lubricated bearings and seals by the authors [Refs. 1-7] have yielded most of the generalized characteristics discussed and used in this paper. They include bearing and seal nonlinear fluid film properties associated with stiffness, damping, and fluid average circumferential velocity ratio. Analytical relationships yield the rotor system's dynamic stiffness characteristics. This paper shows the combination of these data to provide the fluid-induced rotor stability equations.

NOMENCLATURE

C	Bearing or seal radial clearance
D	Fluid film radial damping
D_s	Shaft modal damping coefficient
e	Shaft eccentricity ratio
$\bar{F}_{pert\ z}$	Circular perturbation force vector
j	$\sqrt{-1}$
K, K_1, K_2	Rotor modal stiffnesses
K_B	Fluid film direct (radial) stiffness
K_{Bo}	Fluid film direct (radial) stiffness for concentric shaft
K_D, K_Q	Rotor system direct and quadrature dynamic stiffnesses respectively
M	Rotor modal mass
M_{fl}	Fluidic inertia effect
$\bar{z}=x+jy$	Rotor lateral displacement (x--horizontal, y--vertical)
α	Force/response phase angle for periodic perturbation
η	Fluid viscosity
λ	Fluid circumferential average velocity ratio
λ_o	Fluid circumferential average velocity ratio for concentric shaft
ω	Precession frequency
ω_{ASY}	Asymptotic value at whip precession frequency
ω_{th}	Precession frequency at threshold of stability
Ω	Rotative speed

RESULTS OF PERTURBATION TESTING OF ROTORS IN BEARINGS AND SEALS

Dynamic stiffness properties of rotor systems are studied by applying a perturbation force of sinusoidal nature to a rotor. The best results are obtained when the force is circular (sinusoidal in two orthogonal lateral directions) and applied in a plane perpendicular to the shaft axis. The rotor is held at a constant speed while the perturbation force frequency is varied from zero to frequencies well above the rotative speed, in either forward (the same direction as shaft rotation) or reverse direction (opposing rotation). The frequency, amplitude, and phase of the perturbation force is accurately documented. The amplitude and phase of the displacement response of the rotor at each perturbation force frequency is then carefully measured. Dividing the perturbation force vectors by the corresponding response vectors yields the dynamic stiffness vectors. Plotting these dynamic stiffness vectors in terms of their direct and quadrature components across wide perturbation frequency ranges allows dissection and evaluation of the dynamic stiffness components [Refs. 1,2,4,5].

In classical rotor dynamics for laterally isotropic systems, the bearing or seal fluid film direct dynamic stiffness terms are referred to as combination of direct (radial) spring, cross damping, and direct mass. The quadrature dynamic stiffness contains cross spring, direct (radial) damping, and cross mass. (Laboratory observations up to this time, however, reveal no cross mass term.)

The authors use the same definitions, but there are the following adjustments: (a) direct spring is shown to be a sum of the fluid film hydrodynamic stiffness plus the hydrostatic (externally pressurized) stiffness minus a component associated with the fluidic inertia effect; (b) cross damping is shown to be a component of the fluidic inertia effect; (c) the direct mass term is a component of the fluidic inertia effect; and (d) cross spring is a product of the direct damping, circumferential average velocity ratio, and rotative speed.

For a particular seal or bearing operated at low eccentricity at a particular rotative speed, with a specific fluid at a known temperature (for knowledge of viscosity), the results of the combination of a forward and reverse perturbation runs typically yield the direct dynamic stiffness and quadrature dynamic stiffness curves as shown in figure 1. Additionally, a steady-state load test can be used to better evaluate the stiffnesses at a zero perturbation (precession) frequency (ω=0) [Ref. 2].

The general expressions of the fluid dynamic force components applied to the rotor with a coordinate system of +Y up and +X right and counterclockwise (X toward Y) rotation are

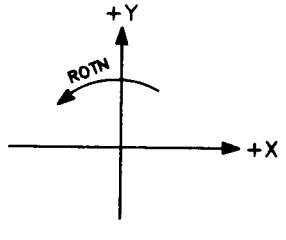

$$\begin{bmatrix} F_x \\ F_y \end{bmatrix} = \begin{bmatrix} K_{xx} & K_{xy} \\ -K_{yx} & K_{yy} \end{bmatrix} \begin{bmatrix} x \\ y \end{bmatrix} + \begin{bmatrix} D_{xx} & D_{xy} \\ -D_{yx} & D_{yy} \end{bmatrix} \begin{bmatrix} \dot{x} \\ \dot{y} \end{bmatrix} + \begin{bmatrix} M_x & 0 \\ 0 & M_y \end{bmatrix} \begin{bmatrix} \ddot{x} \\ \ddot{y} \end{bmatrix}$$

For sinusoidal isotropic (laterally symmetric) response, due to circular perturbation force $\bar{F}_{pert\ z}$ at frequency ω, the force balance relationship for a concentrically rotating shaft at the bearing or seal is as follows:

$$\bar{F}_{pert\ z} = [K_B-(\omega-\lambda\Omega)^2M_{fl}+jD(\omega-\lambda\Omega)+K-M\omega^2+jD_s\omega]\bar{z} \quad (1)$$

where:

$\bar{z}=x+jy$ is rotor lateral response vector at frequency ω.

$\bar{F}_{pert\ z}$ is the perturbation force vector of the sinusoidal circular nature.

K_B is the sum of the hydrodynamic plus the hydrostatic (externally pressurized) bearing/seal fluid film direct (radial) stiffness (the nonlinear character of this term as a function of shaft eccentricity is a vital relationship for the rotor stability solution.

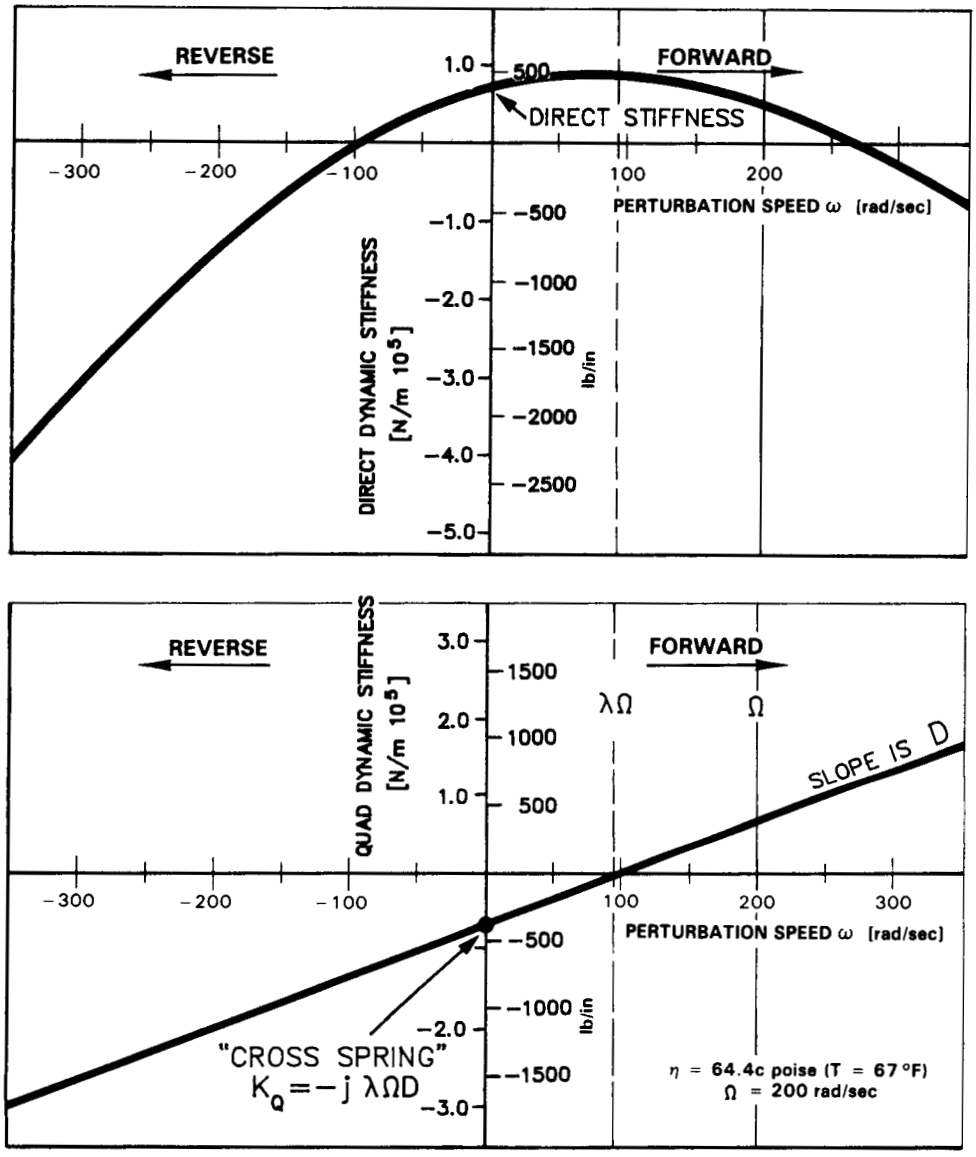

FIGURE 1 TYPICAL SEAL OR BEARING FLUID FILM DYNAMIC STIFFNESS PLOTS VERSUS PERTURBATION FREQUENCY FOR FORWARD AND REVERSE PERTURBATION. DIRECT DYNAMIC STIFFNESS CONTAINS STATIC RADIAL (DIRECT) STIFFNESS AND INERTIA TERMS. QUADRATURE DYNAMIC STIFFNESS CONTAINS RADIAL DAMPING AND "CROSS SPRING" TERMS (SHAFT DAMPING NEGLECTED).

j is $\sqrt{-1}$.

ω is sinusoidal perturbation frequency (+ for forward, - for reverse). Later, this same term means also rotor precession rate when instability (stable limit cycle, fluid-induced whirl or whip) occurs.

D is fluid film direct (radial) damping.

λ is the average circumferential component of fluid flow ratio to rotative speed in the seal, bearing, or rotor periphery. It is also the rate at which the fluid dynamic force rotates. It has been described in prior publications [Refs. 5-11]. Most authors assume that this rate is 1/2 [Refs. 14-16]. The major change and improvement documented by the authors is that λ is not constant and, in particular, is a nonlinear, decreasing function of the shaft eccentricity.

Ω is rotor rotative speed.

M_{fl} is a synthetic expression with units of mass, called the fluidic inertia effect.

C is bearing or seal radial clearance.

e is bearing or seal eccentricity ratio $e=|z|/C$.

K,M,D_s are rotor first lateral mode modal (generalized) stiffness, mass, and and external damping respectively.

From (1) the rotor system direct dynamic stiffness is as follows:

$$K_D = (F_{pert\ z}/|z|)\ (\cos\ \alpha) = K_B - (\omega-\lambda\Omega)^2 M_{fl} + K - M\omega^2$$

The quadrature dynamic stiffness is

$$K_Q = -(F_{pert\ z}/|z|)\ (\sin\ \alpha) = D(\omega-\lambda\Omega) + D_s\omega$$

where α is angle between the perturbation force and rotor response vectors.

Expanding the binominal terms of the fluidic inertia effect, it may be observed that the fluid-related dynamic stiffness elements are as follows:

(a) $K_{xx} = K_{yy} = K_B - \lambda^2\Omega^2 M_{fl}$, so that the possibility of a "negative spring" exists, as is noted by the authors in prior reports [Refs. 1-5], and is well known to designers and researchers of squeeze film dampers.

(b) $D_{xy} = D_{yx} = +2\lambda\Omega\omega M_{fl}$. It is important to note that this term is positive in nature, as is being now reported by all researchers. This has been reported as a negative term in the 1950 to 1970 era.

(c) $K_{xy} = K_{yx} = \lambda\Omega D$. The "cross" spring is the stiffness of the fluid wedge support term which, as can be observed, is the product of the fluid average circumferential velocity $\lambda\Omega$, times the fluid direct damping D. It results from the rotative character of the fluid dynamic force [Refs. 5,11,14-16]. The term $\lambda\Omega D$ is the key of the rotor stability algorithm.

Two vital characteristics of the fluid inertia effect are

(1) The value of the fluidic inertia effect is zero when the precession speed $\omega=\lambda\Omega$. As most everyone knows, this corresponds, or is near, to one of the conditions of forward fluid-induced instability such as whirl. At the threshold of whirl, the fluidic inertia effect term is, therefore, quite ineffective.

(2) The fluidic inertia effect has the "ghost-like" characteristic because it disappears with increased shaft eccentricity following increasing radial load. Specifically, it is active only as long as circumferential flow is strong and the force from the "cross spring" term is dominant. This occurs at low through medium shaft eccentricities. At high eccentricities the circumferential flow is suppressed, yielding priority to secondary flows (axial and backward [Ref. 10]). At shaft high eccentricities the direct dynamic stiffness terms, mainly the hydrodynamic spring, become dominant and the fluidic inertia effect vanishes.

Due to these characteristics, the fluidic inertia has very little effect on stability threshold or the orbit amplitude and precessional frequency of whirl or whip limit cycles. Therefore, it will be neglected in the following analysis.

NONLINEAR CHARACTERISTICS OF BEARINGS AND SEALS

The next required relationships for determination of rotor stability are nonlinear expressions for the fluid film direct stiffness K_B versus shaft eccentricity, direct damping D versus eccentricity, and the fluid average circumferential flow velocity ratio λ versus eccentricity. It will soon be shown that the only vital nonlinearity affecting the size of whirl or whip limit cycle orbit (rotating eccentricity) is the direct stiffness term. Typical relationships are illustrated in figures 2, 3, and 4. The nonlinear functions of the eccentricity ratio which are taken into consideration are as follows:

$$K_B = \frac{K_{Bo}}{(1 - e^2)^3} \quad , K_{Bo} = 4000 \text{ lb/in} \tag{2}$$

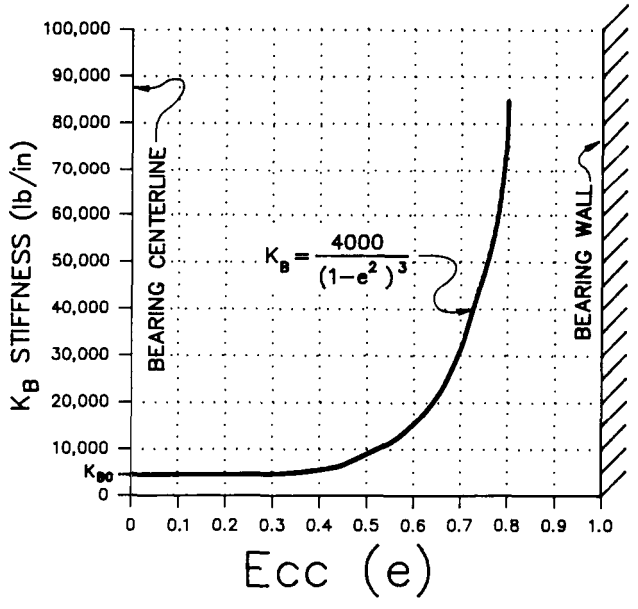

FIGURE 2 TYPICAL FLUID FILM DIRECT (RADIAL) STIFFNESS VERSUS SHAFT ECCENTRICITY RATIO.

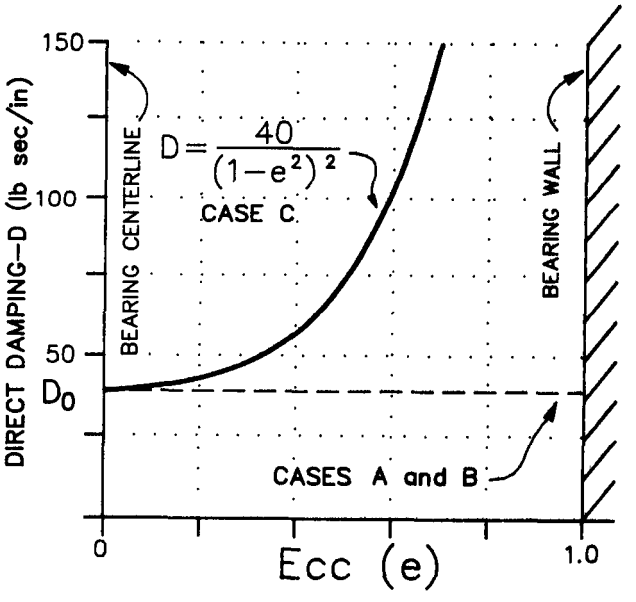

FIGURE 3 TYPICAL FLUID FILM DIRECT (RADIAL) DAMPING VERSUS SHAFT ECCENTRICITY RATIO.

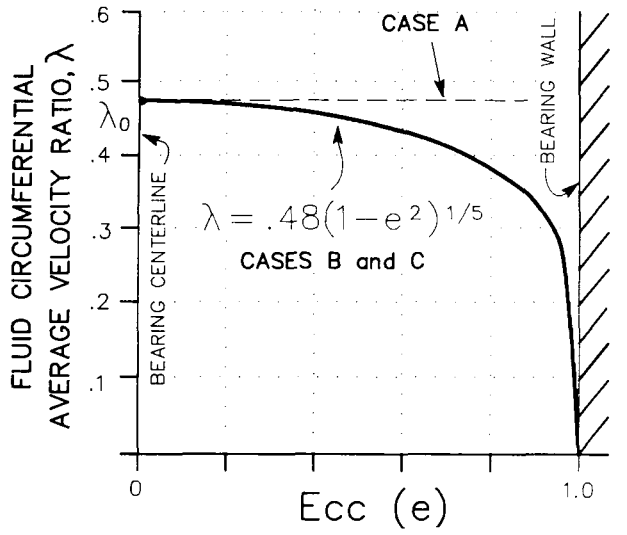

FIGURE 4 TYPICAL FLUID CIRCUMFERENTIAL AVERAGE VELOCITY RATIO VERSUS SHAFT ECCENTRICITY RATIO.

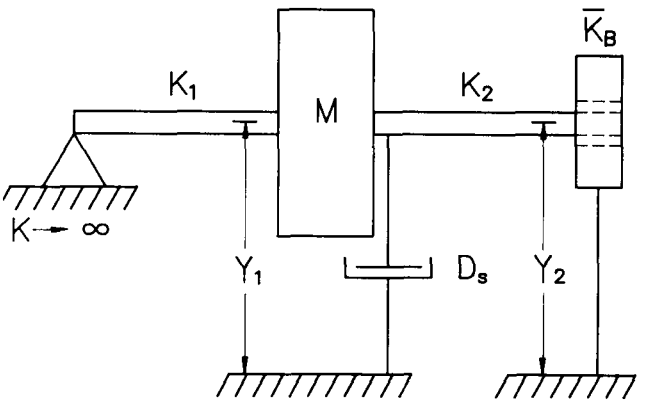

FIGURE 5 ROTOR/BEARING MODEL. THE SIMPLEST SYSTEM DEMONSTRATING WHIRL AND WHIP PHENOMENA.

$$D = \frac{D_o}{(1 - e^2)^2} \quad , D_o = 40 \text{ lb sec/in} \tag{3}$$

$$\lambda = \lambda_o(1 - e^2)^{1/5} \tag{4}$$

These functions qualitatively exemplify the bearing/seal parameter behavior. They are not locked into a specific bearing/seal geometry, dimensions, or Sommerfeld number. K_{B_o}, D_o, and λ_o are fluid film radial stiffness damping and circumferential velocity ratio at concentric shaft respectively.

The experimentally identified variation of λ with eccentricity ratio is noted in the prior reports [Refs. 7, 9, 11]. No clean laboratory test has been found for observation of λ at this time, but a few indirect measurements have been accomplished. More numerical/analytical calculations, such as in [Ref. 10], will also help to identify the values of λ as function of eccentricity and other parameters.

ROTOR/BEARING SYSTEM

The final set of equations for determination of stability is the equation of the rotor carrying bearing, seal, or other elements which provide the fluid. A simple rotor supported in one rigid and one fluid lubricated bearing is illustrated in figure 5.

The dynamic stiffness, K_{eq}, observed at the mass M of the rotor system in figure 5 is

$$K_{eq} = K_1 - \omega^2 M + j\omega D_s + \frac{\bar{K}_B K_2}{\bar{K}_B + K_2} \tag{5}$$

where $\bar{K}_B$ is fluid film complex stiffness:

$$\bar{K}_B = K_B + jD(\omega-\lambda\Omega) \tag{6}$$

Thus:

$$K_{eq} = \frac{K_2(K_1-\omega^2M)+K_B(K_1+K_2-\omega^2M)-D_sD(\omega-\lambda\Omega)+j[\omega D_s(K_2+K_B)+D(\omega-\lambda\Omega)(K_1+K_2-\omega^2M)]}{K_2 + K_B + jD(\omega-\lambda\Omega)} \tag{7}$$

In Eq. (7) K_1, K_2 are shaft partial modal stiffnesses (first bending mode); M is rotor modal mass; D_s is shaft modal external damping. Fluidic inertia effect is neglected. More formal analysis of this rotor/bearing system is in [Refs. 3 and 13].

ROTOR STABILITY ANALYSIS

From the standpoint of stability, the numerator of K_{eq} represents poles and the denominator represents zeros. Only those poles are of interest for stability. Further, since only a steady level of the instability limit cycle orbit, if it exists, is of interest, the exponentially increasing and the exponentially decreasing orbits (transient processes) are not discussed. This allows the direct and quadrature parts of the numerator of dynamic stiffness K_{eq} (the denominator of dynamic motions) to be separated and set to zero individually to find the stability roots. Another way to state this, is that the roots are evaluated at log decrement of zero. From control theory backgrounds, the root locus shown in figure 6 is solved only when the direct (real) parts of the roots are zero. The corresponding quadrature value is the precession rate, leading the system to the limit cycle of whirl or whip.

Liapounoff contributed strongly to the study of stability. One of his theorems noted in [Ref. 17] is

> "Liapounoff's theorem states that under certain conditions which are frequently encountered in physical problems, the information obtained from the linear equations of the first approximation is sufficient to give a correct answer to the question of stability of the nonlinear system."

Restated, the linear portions of the direct and quadrature stiffness K_{eq} solved for their roots yield the answer to the first problem of stability. Once the question of stability is decided, the next step is to evaluate the amplitude of the limit cycle orbit and rotor precession speed as a function of the nonlinear characteristics.

The direct and quadrature components of Eq. (7) are equalized to zero and solved for K_B and Ω so that

$$K_B = \frac{-K_2(K_1-\omega^2M)(K_1+K_2-\omega^2M)-\omega^2D_s^2K_2}{(K_1+K_2-\omega^2M)^2 + \omega^2D_s^2} \tag{8}$$

and

$$\Omega = \frac{\omega}{\lambda}\left[1 + \frac{D_sK_2^2}{D[(K_1+K_2-\omega^2M)^2 + \omega^2D_s^2]}\right] \tag{9}$$

The right-hand side expression of Eq. (8) for various precession rates, omitting the minor terms with D_s, is illustrated in figure 7.

EXAMPLES

In order to plot the precession speed ω against the rotative speed Ω for a particular case, it is necessary to choose values and functional relationships for the various rotor system parameters. The most simple process of solving the problem is to step the eccentricity ratio "e" gradually from 0 to about 0.9. For each eccentricity the values of K_B, D, and λ are calculated from appropriate equations such as Eqs. (2), (3), (4). Eq. (8) is then solved for the precession ω associated with corresponding eccentricity ratio e. Finally, for each rotative speed Ω, the size of the limit cycle whirl/whip orbit eC (where C is bearing or seal radial clearance), and the speed of precession ω, are all established.

As an example, for CASE A the nonlinear terms are stated as follows:

$$K_B = \frac{K_{Bo}}{(1-e^2)^3} \quad , \qquad K_{Bo} = 4000 \text{ lb/in (fluid film radial stiffness at concentric shaft)} \tag{10}$$

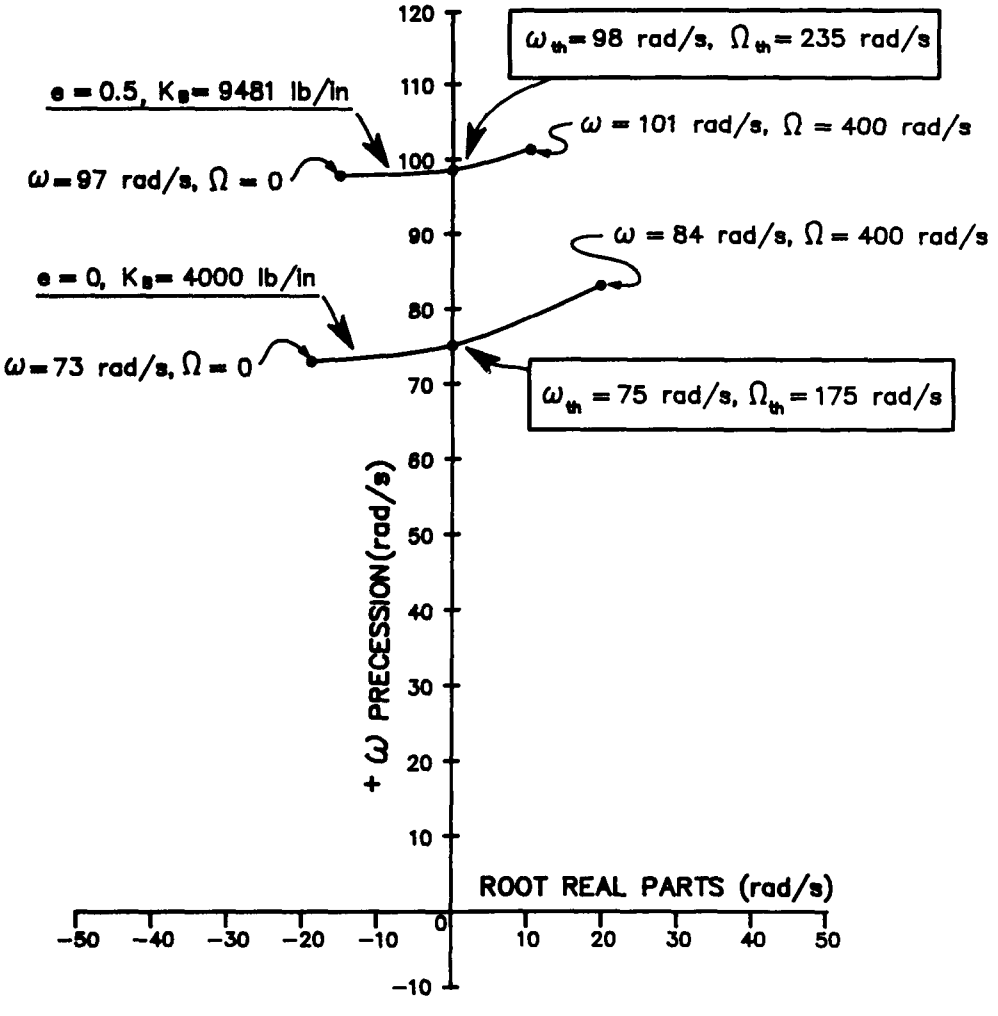

FIGURE 6 EXAMPLE OF ROOT LOCUS OF THE WHIRL/WHIP ROOT (ω_{th} IS THRESHOLD OF STABILITY).

$$D = D_0 = 40 \text{ lb sec/in (constant for this case)} \tag{11}$$

$$\lambda = \lambda_0 = 0.48 \text{ (constant for this case)} \tag{12}$$

The remaining parameters are chosen as

$$\begin{aligned} K_1 &= 2000 \text{ lb/in} & M &= 1.0 \text{ lb sec}^2/\text{in} \\ K_2 &= 38000 \text{ lb/in} & D_s &= 4.0 \text{ lb sec/in} \end{aligned} \tag{13}$$

The graph of the precession frequency of the whirl and whip against the rotative speed is shown in figure 8. This figure also shows the whirl and the whip ranges, and the smooth transition region between whirl and whip. It also shows a few corresponding whirl and whip orbits at the bearing (or seal) with their magnitude and frequency, as well as the stability threshold and asymptotic frequency.

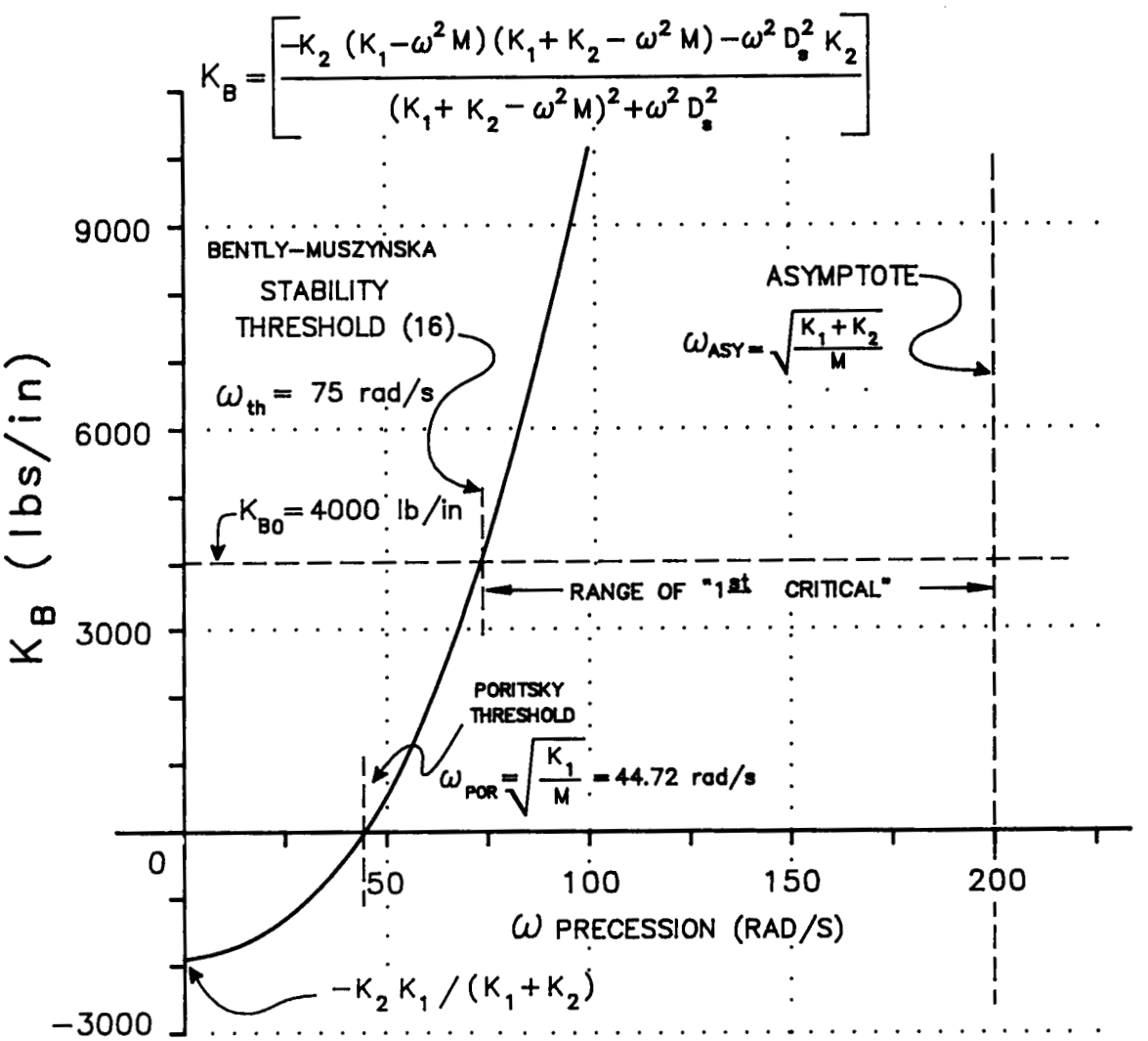

FIGURE 7 RIGHT-HAND SIDE EXPRESSION OF EQUATION (8) VERSUS PRECESSION RATE. EQUATIONS (10) TO (13) INDICATE VALUES OF PARAMETERS USED IN THIS EXAMPLE.

Figure 8 also illustrates the result of CASE B, where λ is no longer considered constant, but $\lambda = 0.48\ (1\text{-}e^2)^{1/5}$. The result is virtually the same as CASE A, with constant λ.

For CASE C, damping is no longer constant but equals $D = \frac{40}{(1\text{-}e^2)^2}$. It may be noted in figure 8 that the whirl/whip frequency of CASE C is much more like practically observed behavior, much closer to the asymptotic frequency, which is natural, because damping is always a nonlinear term.

From Eq. (9) the ratio of the precession rate ω to rotative speed rate Ω is an intrinsic function of ω:

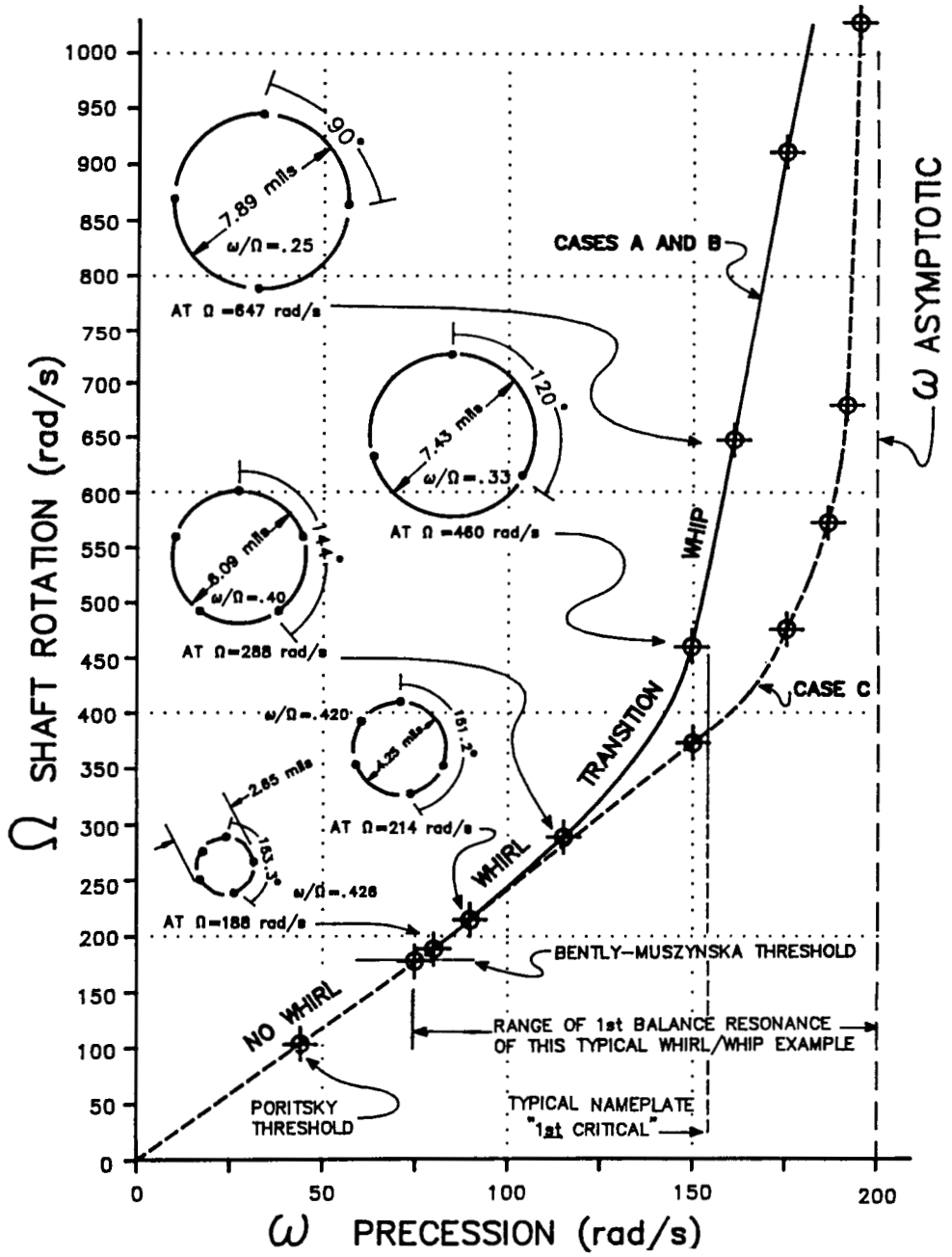

FIGURE 8 ROTATIVE SPEED VERSUS WHIRL/WHIP PRECESSION FREQUENCY FOR THE ROTOR ILLUSTRATED IN FIG. 1 (C = 5 MILS, SHAFT CENTERED). WHIRL/WHIP ORBITS.

$$\frac{\omega}{\Omega} = (\lambda)\left[\frac{1}{1 + \frac{D_s K_2^2}{D[(K_1+K_2-\omega^2M)^2 + \omega^2D^2]}}\right] \tag{14}$$

The shaft damping D_s has a fair amount of control over the actual precession frequency ω to rotative speed Ω as shown in Eq. (14), but has very little control over the right-hand side expression in Eq. (8). Therefore, dropping shaft damping D_s from Equation (8) and solving the equation for precession rate ω yields

$$\omega \approx \left[\frac{K_1K_2 + K_B(K_1+K_2)}{(K_B + K_2)M}\right]^{1/2} \tag{15}$$

The lowest precession rate ω_{th} that the whirl or whip can have, is at the minimum K_B, which is at K_{Bo} for the case of the shaft centered in the seal or bearing considered in this paper. Therefore, in terms of precession frequency ω, the threshold of stability is

$$\omega_{th} \approx \left[\frac{K_1K_2 + K_{Bo}(K_1+K_2)}{(K_{Bo} + K_2)M}\right]^{1/2} \tag{16}$$

Poritsky [Ref. 18] nearly had this threshold more than thirty years ago. He showed the rotative speed whirl threshold at $2\sqrt{K_1/M}$. That is excellent for that time. Note that if bearing stiffness $K_B = 0$, shaft damping $D_s = 0$, and $\lambda_o = 1/2$ and thus $\Omega = 2\omega$, it would be right on. His paper apparently was subjected to very heavy criticism, so his excellent work was not pursued. The authors privately call the zero bearing stiffness threshold the "Poritsky threshold." It is useful to observe that if the outboard shaft stiffness K_1 (the portion of shaft away from the fluid lubricated bearing) becomes very soft (approaches zero), whirling may occur at extremely low rotative speeds. The authors demonstrated a laboratory model with this phenomenon for several years before fully understanding its rules of behavior.

The asymptotic frequency ω_{ASY} occurs as rotative speed increases so that the shaft orbit takes up most of the clearance, and eccentricity ratio e approaches 1. The limit occurs not with nonlinear terms λ or D, but with bearing stiffness K_B which goes to extremely high values at high eccentricity so that for Eq. (15)

$$\omega_{ASY} = \omega|_{e\to 1} = \sqrt{(K_1+K_2)/M} \tag{17}$$

It should be noted that shaft damping D_s was assumed to be 0 for Eq. (15). If shaft damping D_s is high enough, it is possible for the rotor system to escape whipping as shown in [Refs. 12 and 13]. Virtually most documented cases from actual machinery, however, exhibit the asymptotic behavior.

OBSERVATIONS AND CONCLUSIONS

There are numerous straightforward observations available from these stability algorithms.

First, while the "criticals" of machinery are often posted on the nameplate as a fixed frequency, it is obvious that they vary widely due to the nonlinear stiffness of fluid film in bearings and seals. The whirl/whip root of Eq. (8) shows clearly that the resonance ("critical") varies from the threshold to the asymptotic frequency ω_{ASY} as a function of the nonlinear stiffness K_B. In the examples shown, it varies from the threshold of 75 rad/sec (716 rpm) to the asymptotic frequency of 200 rad/sec (1909 rpm) (Figure 8). This fact will probably be met with considerable disbelief, until the nature of the fluid-induced whirl and whip instabilities become more widely understood.

Since both of the quadrature dynamic stiffness elements contain the direct damping term: $K_Q = \omega D - \lambda\Omega D$ the magnitude of the direct damping D has very little effect on stability for rotors operating at low eccentricity. This means that large direct damping D does not create stability.

Direct damping D is well known to be a function of bearing or seal geometry and physical dimensions. It also varies directly with lubricant viscosity η. However, it is not the viscosity in direct damping D which influences stability. It is the influence of viscosity in the hydrodynamic, as well as the hydrostatic (externally pressurized) portions of the bearing or seal stiffness term K_B that exhibits influence on stability.

It is already known that antiswirling mechanisms which suppress the strength of circumferential flow and drive the fluid average circumferential velocity ratio λ as nearly as possible to zero are the proper prevention of fluid-induced whirl and whip [Ref. 6].

Reasonably well known is that forward preswirling of the fluid will drive the precession to rotation ratio to higher values [Ref. 6], sometimes well above half rotative speed. A report on a pump [Ref. 19] with a whirl which tracked about 80% of rotative speed was presented recently. Another verbal report [Ref. 20] on a double volute pump on an offshore platform noted a whirl which tracked 75% of rotative speed. A double driven generator connected by hydraulic clutches with two gas turbines exhibited subsynchronous vibrations with frequency 82.5% to 89.7% of the rotative speed when the clutches were not entirely engaged [Ref. 21]. An "inside-out" bearing with a hollow shaft rotating around a stationary post, will produce λ of slightly over 1/2 [Ref. 22].

The pump with seal whirl [Ref. 19] was most unusual, because nearly all rotor/seal systems exhibit whip only. With good probability, this is because there is a much softer spring K_1 in that pump. Usually when the seal is involved, the stiffness K_1 is much higher. It may be noted in the discussed example that an increase of the magnitude of K_1 leads to the increase of the inception threshold of stability.

It is reasonably well known that any force which moves the rotor to high dynamic eccentricity, thus raising bearing or seal stiffness, can prevent whirl or whip. This action and the stability thresholds due to the unbalance force excitation were previously published [Ref. 3].

It is also well known that steady-state sideload forces, which move the rotor to static high eccentricity in the seal or bearing, are a pallative for fluid-induced instability. Newkirk [Ref. 23] made the first pressure dam bearing for that purpose in 1934. Deliberate sideloading (often by gravity for horizontal rotors) is a very popular "fix" for stability.

Two errors of first magnitude correlated to steady-state sideloads occur. The first is the rule that "the heavier the rotor, the better the stability," which has been published (and apparently believed) for over 30 years. As can be observed from the stability algorithms, the more the rotor mass, the worse the stability for the shaft-centered case. However, since the rule surely was meant to apply to horizontal rotors in the gravity of earth, having more mass means more weight, resulting in higher eccentricity, and thus higher K_B, yielding the better stability. (This assumes no other steady-state sideloading forces, such as caused by misalignment, which adds or subtracts from the gravity load.) Two stabilizing and destabilizing factors, namely the weight-related preload and the added mass, are both very effective, so that which factor wins depends upon the particular conditions in each particular case. A formula for stability that utilizes clearance and rotor weight should be carefully avoided, no matter how popular it has been.

The second big problem of a steady-state sideload application occurs when the rotor is stacked (not integral), consisting of shrink-on wheels or, especially, when the rotor is bolted together (known as a shish ke-bab design). The bowing resulting from the steady sideloading strongly activates the hysteretic internal friction. Thus, attempts to sideload the rotor may help reduce the fluid-induced instability by raising K_B, but get the rotor into an even worse problem of hysteretic friction instability, plus possible rotor-to-stator rubs.

There exists another rule which is incorrectly applied by rotating machinery users. It states: "For stability maintain oil pressure low." This rule generally holds true when the bearing has a partial fluid film (180 degrees as opposed to 360 degrees lubrication). As long as the partial film is maintained, a regular circumferential flow pattern is not established so that stability is assured. To maintain partial lubrication, the pressure should be kept low; otherwise the bearing becomes fully lubricated with stronger circumferential flow, which makes the rotor susceptible to instability. The rule, "Keep oil pressure low," became however, universal, and thus often incorrectly applied. Experimental evidences, as well as the conclusions from the stability algorithm discussed in this paper, show clearly that fluid higher pressure, which directly increases the fluid film radial stiffness K_B, improves rotor stability.

An interesting sidelight is that with the discussed stability algorithm it is simple to get some idea of how much torque is developed by the whirl/whip instability action. With a shaft radius R, and whirl or whip orbit radius eC:

Wedge Stiffness	$\lambda\Omega D$	lb in	Whirl/Whip Torque	$\lambda\Omega DeCR$	lb in
Tangential Force	$\lambda\Omega DeC$	lbs	Whirl/Whip Power Loss	$\lambda\Omega DeCR\omega$	lb in/sec

For $\lambda = 0.5$, $\Omega = 250$ rad/sec, D = 40 lb sec/in, e = 0.5, C = 0.01 inch, and R = 10 inches, the whirl/whip torque is 250 lb/in, and the power loss at precession frequency 124 rad/s is 31000 lb in/sec.

Finally, the fluid dynamic force relationships discussed in this paper can successfully be used in modelling more complex rotor/bearing/seal systems [Refs. 9,12, 13,22]. The model predicts existence of several whirl/whip regimes and explains

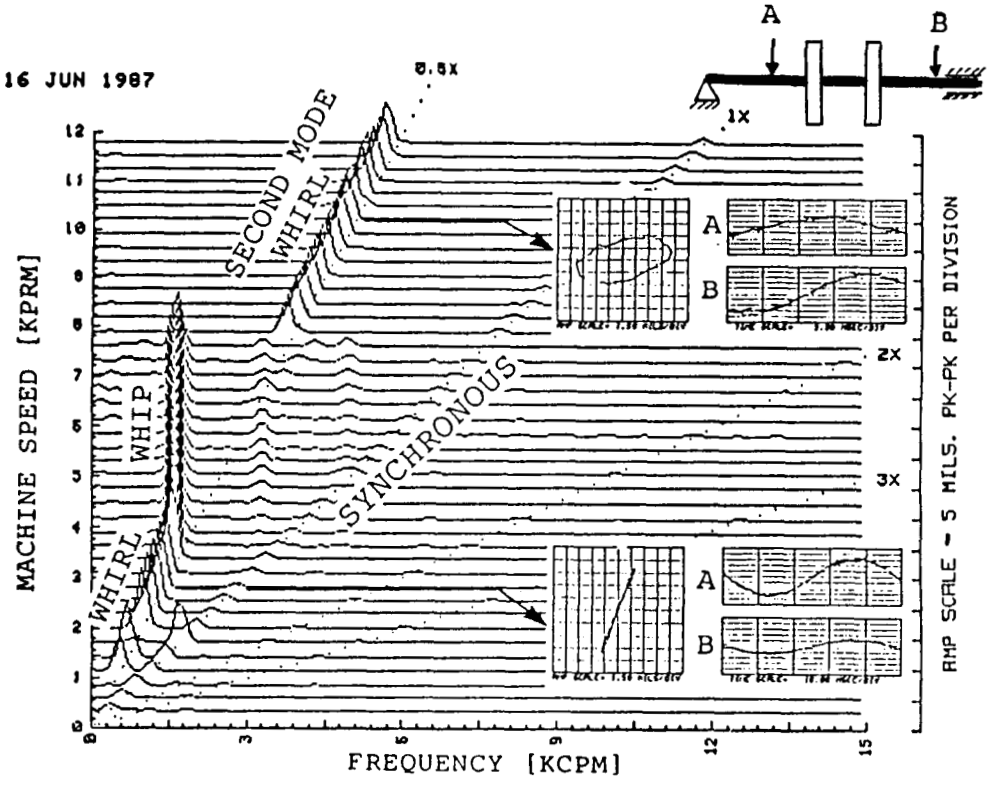

FIGURE 9 SPECTRUM CASCADE OF THE ROTOR VIBRATIONAL RESPONSE DURING START-UP, MEASURED BY THE PROXIMITY TRANSDUCER "B." THE PLOT SHOWS A "JUMP" OF SELF-EXCITED VIBRATIONS FROM WHIP MODE TO THE SECOND MODE WHIRL (JUMP IN AMPLITUDE AND FREQUENCY). THE SKETCH INDICATES TRANSDUCER LOCATIONS. OSCILLOSCOPE IN ORBITAL MODE FOR SIGNALS FROM TRANSDUCERS A AND B DISPLAYS THAT SHAFT AT LOW SPEED WHIRL VIBRATES IN PHASE. AT HIGH SPEED WHIRL SHAFT VIBRATES AT ITS SECOND MODE (RIGHT- AND LEFT-HAND SIDE SHAFT SECTIONS ARE 90 DEGREES OUT OF PHASE).

the "jump" phenomenon observed on laboratory rigs and shown in figure 9, as well as in reported field data (figure 10).

The role of the fluid circumferential flow in rotor stability is emphasized. The fluid average circumferential velocity ratio is the key factor of the "cross spring" term, which, in turn, represents a portion of the quadrature dynamic stiffness: $K_Q = D(\omega-\lambda\Omega)$. The value $\lambda\Omega$ used to be referred to as "bearing resonance" across half a century. While this resonance is hidden in synchronous perturbation tests, it is clearly exposed by nonsynchronous perturbation testing [Ref. 1-5]. An increase of the circumferential flow strength leads to an increase of λ, thus a decrease of the quadrature stiffness of the system. When at the same frequency both K_Q and direct dynamic stiffness K_D equal zero, the instability occurs. This was shown on the root locus of figure 6. The quadrature dynamic stiffness, combined with the nonlinear bearing (or seal) stiffness in the rotor system equation, provides the reliable stability prediction formulas.

REFERENCES

1. Bently, D. E., Muszynska, A., Perturbation Study of Rotor/Bearing System: Identification of the Oil Whirl and Oil Whip Resonances. Tenth Biennial ASME Design Engineering Division Conference on Mechanical Vibration and Noise, 85-DET-142, Cincinnati, Ohio, September 1985.

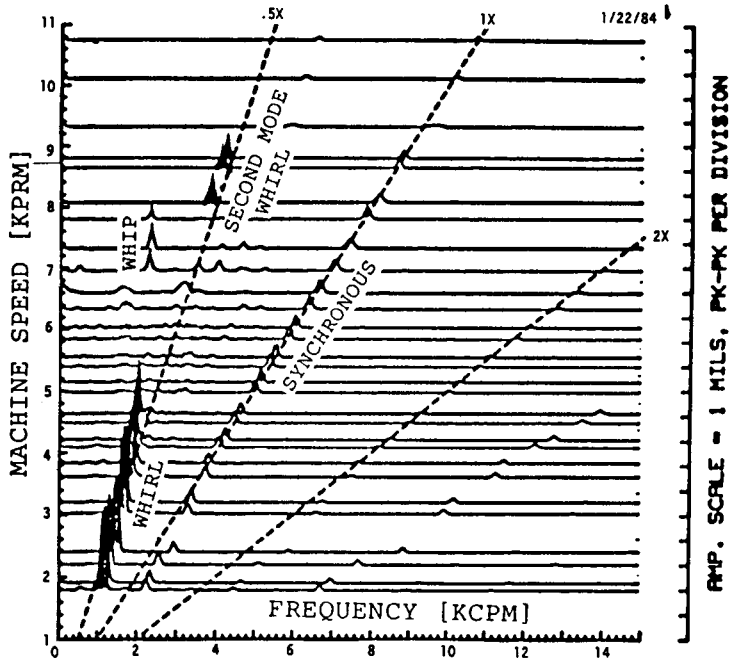

FIGURE 10 SPECTRUM CASCADE OF VIBRATION RESPONSE OF A STEAM TURBINE DRIVEN COMPRESSOR. THE PLOT INDICATES THE WHIRL, WHIP, AND SECOND MODE WHIRL. COURTESY OF C. JACKSON.

2. Bently, D. E., Muszynska, A., Identification of Bearing and Seal Dynamic Stiffness Parameters by Steady-State Load and Squeeze Film Tests. Proc. of BRDRC Symposium on Instability in Rotating Machinery, Carson City, Nevada, NASA Conf. Publ. 2409, 1985.

3. Muszynska, A., Whirl and Whip -- Rotor/Bearing Stability Problems. Journal of Sound and Vibration, Vol. 110, No. 3, 1986.

4. Bently, D. E., Muszynska, A., Modal Testing and Parameter Identification of Rotating Shaft/Fluid Lubricated Bearing System, 4th International Modal Analysis Conference Proceedings, Los Angeles, California, February 1986.

5. Muszynska, A., Modal Testing of Rotor/Bearing Systems, International Journal of Analytical and Experimental Modal Analysis, July 1986.

6. Bently, D. E., Muszynska, A., Anti-Swirl Arrangements Prevent Rotor/Seal Instability. Thermo-Fluid Dynamics of Rotating Machinery. Proc. of 2nd ASME-JSME Thermal Engine Conference. Honolulu, Hawaii, March 1987.

7. Bently, D. E., Fluid Average Circumferential Velocity Ratio a Key Factor in Rotor/Bearing/Seal Models. Orbit, BNC, Vol. 8, No. 1, February 1987.

8. Muszynska, A., Tracking the Mystery of Oil Whirl. Sound and Vibration, February 1987.

9. Muszynska, A., Improvements in Lightly Loaded Rotor/Bearing and Rotor/Seal Models. Rotating Machinery Dynamics, ASME Publ. #H0400A, 11th Biennial ASME

Design Engineering Division Conference on Vibration and Noise, Boston, Massachusetts, September 1987.

10. Tam, L. T., Przekwas, A. J., Muszynska, A., Hendricks, R. C., Braun, M. J., Mullen, R. L., Numerical and Analytical Study of Fluid Dynamic Forces in Seals and Bearings. Rotating Machinery Dynamics, ASME Publ. #H0400B, 11th Biennial ASME Design Engng. Div. Conf. on Vibration and Noise, Boston, Massachusetts, September 1987.

11. Muszynska, A., Fluid-Related Rotor/Bearing/Seal Instability Problems. Bently Rotor Dynamics Research Corporation Report, 1986.

12. Muszynska, A., Multi-Mode Whirl and Whip in Rotor/Bearing Systems. Proc. of the 2nd International Symposium on Transport Phenomena, Dynamics, and Design of Rotating Machinery, Honolulu, Hawaii, April 1988.

13. Muszynska, A., Stability of Whirl and Whip in Rotor/Bearing Systems. Journal of Sound and Vibration, to appear.

14. Bolotin, V. V., Nonconservative Problems in Elastic Stability Theory (in Russian), Gos. Isd. Fiz. Mat. Lit, Moskva, 1961.

15. Black, H. F., Effects of Hydraulic Forces in Annular Pressure Seals on the Vibrations of Centrifugal Pump Rotors. Journal of Mechanical Engineering Science, Vol. II, No. 2, 1969.

16. Black, H. F., Jensen, D. N., Dynamic Hybrid Bearing Characteristics of Annular Controlled Leakage Seals. Proceedings Journal of Mechanical Engineering, Vol. 184, 1970.

17. Minorsky, N., Introduction to Non-Linear Mechanics. Edwards, Y. W., Ann Arbor, 1947.

18. Poritsky, H., Contributions to the Theory of Oil Whip. Trans. ASME, Vol. 75, No. 6, 1953.

19. Massey, I., Subsynchronous Vibration Problems in High-Speed, Multistage Centrifugal Pumps, 14th Texas A&M Turbomachinery Symposium, 1985.

20. Ryan, T., Phillips Petroleum, Private Communications.

21. Franklin, D. E., Van Horne, J. C., Dynamic Analyses of an Over-Running Clutch Vibration Problem on a Gas Turbine Generator Set. Proc. of the Eighth Machinery Dynamics Seminar, NRC Canada, Halifax, Nova Scotia, 1984.

22. Muszynska, A., Bently, D. E., The Role of the Circumferential Flow in Rotor/Bearing/Seal System Stability. Sixth Annual ROMAC Vibration Short Course, 1988.

23. Newkirk, B. L., Grobel, L. P., Oil-Film Whirl--A Non-Whirling Bearing, APM-56-10, 1934.